3-in-1 Transporters Hot Paper

How to cite: *Angew. Chem. Int. Ed.* **2021**, *60*, 12924–12930
International Edition: doi.org/10.1002/anie.202101489
German Edition: doi.org/10.1002/ange.202101489

Crystal Packing-Guided Construction of Hetero-Oligomeric Peptidic Ensembles as Synthetic 3-in-1 Transporters

*Jie Shen, Ruijuan Ye, and Huaqiang Zeng**

Abstract: *Strategies to generate heteromeric peptidic ensembles via a social self-sorting process are limited. Herein, we report a crystal packing-inspired social self-sorting strategy broadly applicable to diverse types of H-bonded peptidic frameworks. Specifically, a crystal structure of H-bonded alkyl chain-appended monopeptides reveals an inter-chain separation distance of 4.8 Å dictated by the H-bonded amide groups, which is larger than 4.1 Å separation distance desired by the tightly packed straight alkyl chains. This incompatibility results in loosely packed alkyl chains, prompting us to investigate and validate the feasibility of applying bulky tert-butyl groups, modified with an anion-binding group, to alternatively interpenetrate the straight alkyl chains, modified with a crown ether group. Structurally, this social self-sorting approach generates highly stable hetero-oligomeric ensembles, having alternated anion- and cation-binding units vertically aligned to the same side. Functionally, these hetero-oligomeric ensembles promote transmembrane transport of cations, anions and more interestingly zwitterionic species such as amino acids.*

Introduction

Aside from serving as the main building blocks for protein synthesis, amino acids are also involved in a myriad of biochemical pathways and physiological processes, including nucleotide biosynthesis, DNA methylation, cellular signaling, activation of mechanistic target of rapamycin, cytoprotection against cell death, cellular transformation, learning, memory, etc.[1–10] In cells or cellular organelles, homeostatic balance in amino acid composition is maintained by at least sixty specialized amino acid transporters (AATs) in a sophisticated manner.[8] Dysregulated AATs could lead to homeostatic imbalance and metabolic reprogramming. These contribute to many forms of human diseases and the pathogenesis of cancer.[8–10] Synthetic amino acid transporters, which may be used to complement or replace the malfunctioned AATs to ensure regulated delivery of required amino acids, may offer tangible therapeutic benefits.

Nevertheless, over the past four decades of intensive research since the first report on the synthetic transporter in 1982,[11] study on the synthetic membrane transporters has overwhelmingly focused on transport of inorganic cations[12–37] or anions,[38–60] with much less on molecular species such as water[61–71] and glucose.[72] Specific to synthetic amino acid transporters, we are aware of only two artificial transporter systems based on a pillar[5]arene derivative by Hou in 2013[73] or dynamic covalent bonds by Gale in 2015.[74]

In 2017, we demonstrated a modularly tunable molecular strategy toward rapid evolution of highly K^+-selective channels.[26] In this strategy, cation-binding and -transporting crown either units were vertically aligned to the same side using a monopeptide-based H-bonded scaffold, generating cation-transporting channels such as **6V10** (Figure 1a). To unambiguously confirm that these crown ethers were indeed aligned to the same side, we have made extensive and combinatorial attempts to grow the X-ray quality single crystals over a long period of two years, eventually and very recently giving rise to single crystals of **6V10** by dissolving it in DMSO at 10 mM and allowing the crystals to slowly grow at room temperature over three months. The crystal structure of

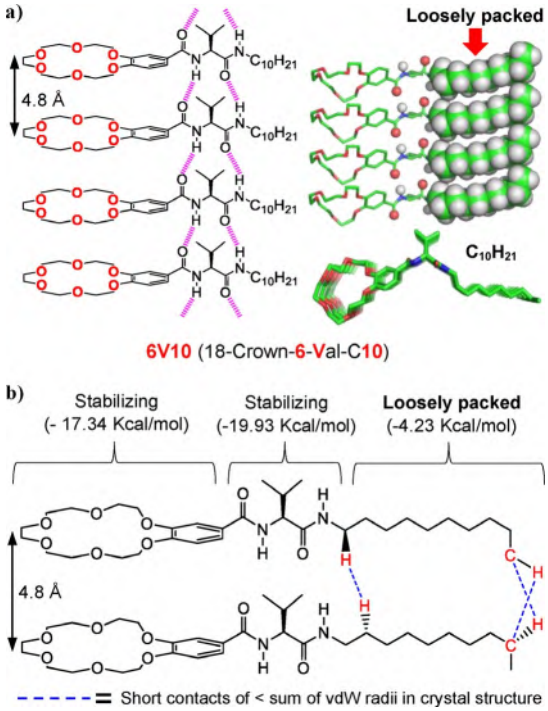

Figure 1. a) Chemical and crystal structures of crown ether-containing K^+-transporting channel 6V10, revealing loosely packed side chains among the decyl chains. b) Computationally calculated binding energies per crown ether group, H-bonding segment and straight decyl chain at the level of ωB97XD/6–311G** in the gas phase for 6V10. Note that a tightly packed docane generates a binding energy of −12.98 Kcal mol^{-1} per molecule.

[*] Dr. J. Shen, R. Ye, Prof. H. Zeng
Department of Chemistry, College of Science, Hainan University
Haikou, Hainan 570228 (China)
E-mail: 2733910004@qq.com

Supporting information and the ORCID identification number(s) for the author(s) of this article can be found under: https://doi.org/10.1002/anie.202101489.

6V10 confirms our early premise, underlying the directional self-assembly of crown ether units that forms a transmembrane pathway for mediating transport of cations (Figure 1a). This directional assembly obviously results from a directional parallel arrangement involving the H-bond-forming amide groups among adjacent mono-peptide scaffolds.

After a more careful inspection of the crystal structure, the most interesting observation perhaps is related to the intermolecular packing. While crown ether groups and H-bonding segments both pack tightly among themselves, each contributing to stabilizing energies of -17.34 kcal mol^{-1} and -19.93 kcal mol^{-1} (Figure 1b), respectively, the straight decyl ($C_{10}H_{21}$) side chains remain essentially non-packed (Figure 1a), with a small overall interaction energy of -4.23 kcal mol^{-1} per chain. This packing energy is 8.75 kcal mol^{-1} less than the binding energy of -12.98 kcal mol^{-1} per tightly packed decane molecule.

This lack of packing among the straight alkyl chains can be readily understood on the basis of molecular dimensionality.

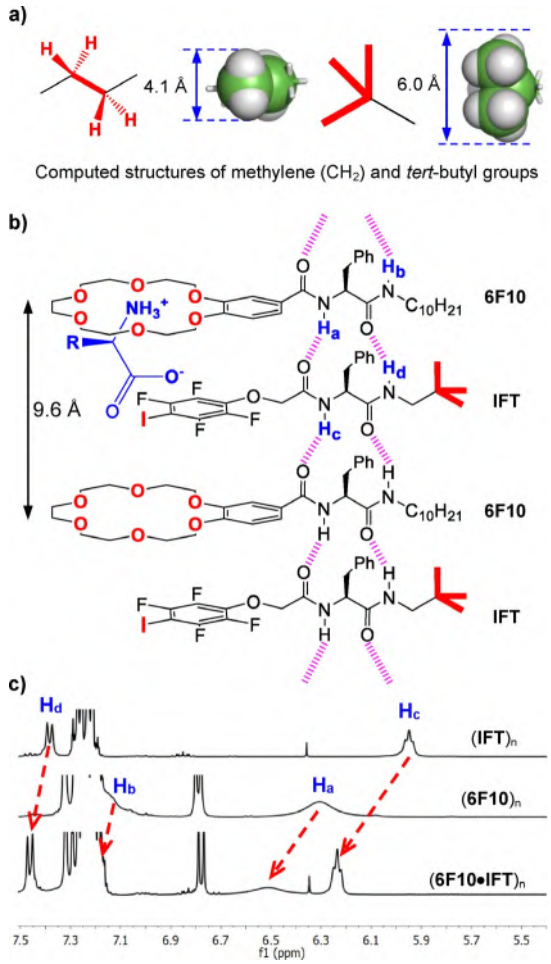

Figure 2. a) Computed molecular dimensionalities for methylene (CH_2) and *tert*-butyl groups at the level of ωB97XD/6–311G**. b) Illustration of applying tert-butyl groups to alternatively interpenetrate the straight alkyl chains, generating more stable hetero-oligomeric peptidic ensembles as three-in-one transporters for transporting cations, anions and amino acids. c) Partial NMR spectra of homo-ensembles $(IFT)_n$ and $(6F10)_n$ and hetero-ensembles $(6F10{\cdot}IFT)_n$, demonstrating the formation of $(6F10{\cdot}IFT)_n$ upon mixing $(IFT)_n$ and $(6F10)_n$.

Specifically, the computed methylene (CH_2) groups of the alkyl chains possess a diameter of 4.1 Å (Figure 2a), which is 0.7 Å smaller than the H-bonding-enforced inter-chain separation distance of 4.8 Å. Thus, existence of some void spaces among vertically aligned alkyl chains is inevitable, a reason why the end methyl group in **6V10** points toward the adjacent alky chain to fill the void as much as possible (Figure 1).

Given a molecular size of 6.0 Å for the *tert*-butyl group (Figure 2a), we envisioned a possibility to interpenetrate one dimensionally aligned alky chains alternatively using the *tert*-butyl groups, forming hetero-ensembles $(6F10{\cdot}IFT)_n$ from homo-ensembles $(IFT)_n$, which likely can transport anions,[52] and $(6F10)_n$, which likely can transport cations,[26] via a social self-sorting process. We further envisioned that ensembles $(6F10{\cdot}IFT)_n$, consisting of alternating cation- and anion-binding motifs, might behave like a three-in-one transporters capable of mediating transmembrane transport of cations, anions and zwitterionic species such as amino acids. Equally significantly, hetero-channel $(6F10{\cdot}IFT)_n$, for the first time, provides an interesting structural tool for quantitatively addressing two fundamentally significant but difficult-to-address issues related to (1) the comparative ion transport efficacies between18-crown-6 and electron-deficient iodo groups and (2) the impact on ion transport activity the inter-chain separation distance and number of binding sites may have.

Results and Discussion

Previously, we have shown that the cation-transporting activities of mono-peptide channels derived from phenylalanine are among the highest and the most selective.

The 1,2,4,5-tetrafluoro-3-iodobenzene motif, which is sterically compatible with the molecular dimensionality of the assembled mono-peptide channel, has been employed to mediate transmembrane anion transport.[75] As a starting point, we therefore decided to examine the pairing compatibility involving decyl-containing 6F10 and *tert*-butyl group-containing IFT (Figure 2b).

It is well-known that H-bond acceptors like N- and O-atoms decrease the electron density of the H-bond donors (H-atoms), producing a deshielding effect and resulting in a larger chemical shift of the H-atoms. The stronger the H-bonds generate stronger deshielding effects and larger chemical shifts. Experimentally, upon mixing homo-ensembles $(IFT)_n$ and $(6F10)_n$ at 100 mM, we observed chemical shifts of all four H-atoms H_a–H_d downfield shifted, with significant differences of 0.20 ppm for H_a, 0.28 ppm for H_c, and 0.07 ppm for H_d. These changes in chemical shift clearly signify the formation of more stable hetero-ensembles $(6F10{\cdot}IFT)_n$ from homo-ensembles $(IFT)_n$ and $(6F10)_n$.

Lastly, the ability of the crown ether and electron-deficient iodide groups to interact with charged ammonium and carboxylate ends of the amino acids was confirmed by ^{1}H and ^{19}F NMR experiments, respectively. Due to the solubility issue of zwitterionic amino acids, we used simple alkyl ammonium (compound **1**; Supporting Information, Figure S1a) and carboxylate (compound **2**; Supporting Informa-

tion, Figure S1b) compounds to represent the ammonium and carboxylate ends of the amino acid. Upon mixing 10 equivalents of compound **1** with 6F10·IFT, the chemical shift of ammonium H-atoms of **1** displays an upfield shift of 0.2 ppm (Supporting Information, Figure S1a), suggesting the binding of ammonium group of **1** by the crown ether of 6F10·IFT. Similarly, in the presence of 10 equivalents of compound **2**, the chemical shift of fluorine atoms of 6F10·IFT displays a downfield shift of 0.4 ppm (Supporting Information, Figure S1b), indicating the binding of carboxylate group by the electron-deficient iodide group of 6F10·IFT. Given the limited cavity size of the crown ether, we believe the most likely scenario concerning amino acid transport involves the binding of the amino acid by 6F10·IFT (Figure 2b), followed by the alternative hopping of the ammonium and carboxylate groups from one binding site to the other.

The main purpose of the following is to fully establish the formation of hetero-ensembles $(6F10{\cdot}IFT)_n$ in solution, exhibiting ion transport behaviors distinctively different from homo-ensembles $(IFT)_n$ and $(6F10)_n$. Based on the hydrophobic membrane thickness of 28 Å for EYPC (egg yolk L-α-phosphatidylcholine) lipid membrane[58] and an inter-chain distance of 4.8 Å in these ensembles, roughly six molecules are required to span the hydrophobic membrane region. Accordingly, we will use $(6F10{\cdot}IFT)_3$, $(IFT)_6$ and $(6F10)_6$ to represent the respective most likely ensembles in the membrane.

The cation transport properties of these three types of ensembles were studied and compared using a pH-sensitive HPTS assay (Figure 3a). This assay relies on the HPTS dye (8-Hydroxypyrene-1,3,6-trisulfonic acid), exhibiting pH-dependent fluorescence at excitation wavelengths of 403 and 460 nm. EYPC lipids were used to prepare large unilamellar vesicles (LUVs) of about 120 nm in diameter in buffer (10 mM HEPES, 50 mM Na_2SO_4, pH 7.0), with intravesicular region encapsulating the pH-sensitive HPTS (1 mM). The HPTS-containing LUV suspension was diluted to the same type of buffer having pH 8.0 to create a pH gradient for ion transport study via Na^+/H^+ antiport mechanism. At the same channel concentration of 7 μM, channel $(6F10{\cdot}IFT)_3$, having a fractional Na^+ transport activity (R_{Na^+}) of 51%, is substantially more active than $(6F10)_6$ (R_{Na^+} = 37%). As expected, the anion-transporting channel $(IFT)_6$ does not transport Na^+ ions, having a R_{Na^+} value of 3.3% that is merely 1% more than the background signal. These data confirm the cation-transporting ability of $(6F10{\cdot}IFT)_3$ to be maintained after enlarging the vertical separation distance between two adjacent crown ether units from 4.8 Å in $(6F10)_6$ to 9.6 Å in $(6F10{\cdot}IFT)_3$. This is consistent with the earlier finding by Fyles, showing that, within a lipid bilayer environment, the maximum distance between two binding sites a sodium ion can travel is 11 Å.[76]

The anion transport properties of $(6F10{\cdot}IFT)_3$ and $(IFT)_6$ were studied and compared using a chloride-sensitive SPQ assay (Figure 3b), taking advantage of the fact that the fluorescence intensity of SPQ dye decreases with increasing concentration of chloride anions. At the same channel concentration of 2 μM, hetero-channel $(6F10{\cdot}IFT)_3$ apparently is more active than anion channel $(IFT)_6$ by 14% in fractional chloride transport. Similarly, these data confirm the anion-transporting ability of $(6F10{\cdot}IFT)_3$ to be maintained after enlarging the vertical separation distance between two

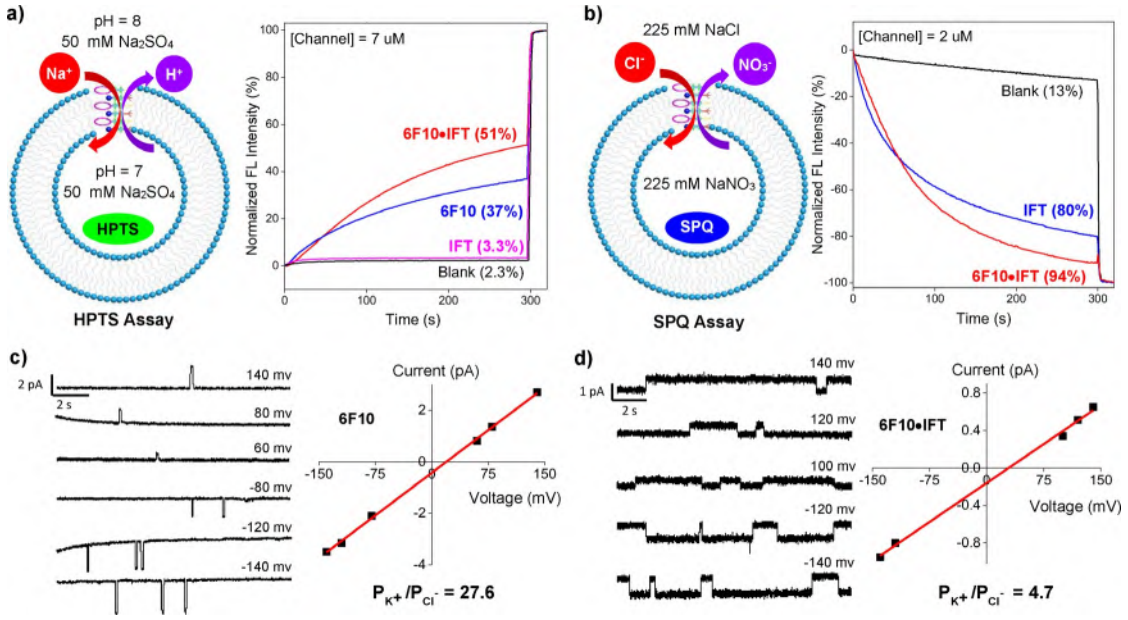

Figure 3. a) pH-sensitive HPTS assay for comparing Na^+ transport activities. b) Chloride-sensitive SPQ assay for comparing chloride transport activities. c) and d) presents single channel currents and K^+/Cl^- selectivity values for home-ensembles $(6F10)_6$ and hetero-ensembles $(6F10{\cdot}IFT)_3$. In (a), the final ion transport trace was obtained, after subtracting background intensity at $t = 0$, as a ratiometric value of I_{460}/I_{403}, and further normalized based on the value of I_{460}/I_{403} after addition of triton. The fractional changes R_H^+ was then calculated for each curve using the normalized value of I_{460}/I_{403} at 300 s before the addition of triton, with that of I_{460}/I_{403} at $t = 0$ s as 0% and that of I_{460}/I_{403} at $t = 300$ s (obtained after addition of triton) as 100%. [total lipid] = 82 μM. In (b), the emission of SPQ was monitored at 430 nm with excitation at 360 nm for 300 s.

adjacent anion-transporting units from 4.8 Å in $(6F10)_6$ to 9.6 Å in $(6F10{\cdot}IFT)_3$.

We have conducted self-quenching carboxyfluorescein (CF, 50 mM) assay to evaluate the membrane integrity in the presence of 6F10·IFT (Supporting Information, Figure S2). While highly fluorescent at low concentration, CF molecules mostly self-quenches at high concentration of 50 mM. Compared to high fluorescence intensities that reach 43% and 95% for melittin at 0.45 and 1.2 μM, 6F10·IFT at 20 μM elicits only $<3\%$ difference relative to the background signal, confirming membrane integrity in the presence of 6F10·IFT and that the observed ion transports are due to the ability of 6F10·IFT to transport these ions.

To quantitatively assess the impacts on ion transport properties (transport rate, selectivity and channel stability) an alternated array of cation- and anion-binding units may have, we conducted single channel current measurements for $(6F10{\cdot}IFT)_3$ and $(6F10)_6$ (Figure 3c,d). There are three noteworthy points to discuss.

First, incorporating anion-binding unit expectedly decreases the K^+/Cl^- selectivity from 27.6 for $(6F10)_6$ to 4.7 for $(6F10{\cdot}IFT)_3$. Still, $(6F10{\cdot}IFT)_3$ behaves mostly like a cation channel, interestingly pointing out a higher ability of the 18-crown-6 in transporting K^+ cations than that of the electron-deficient iodo group in chloride transport. More precisely, the 18-crown-6 group transports K^+ ions 4.7 times as efficient as the chloride transport mediated by the 1,2,4,5-tetrafluoro-3-iodobenzene group. To our best knowledge, this is the first time the relative ion-transporting ability between 18-crown-6 and 1,2,4,5-tetrafluoro-3-iodobenzene motifs has been quantitatively assessed within the identical structural and experimental settings.

Second, if we assume that the currents observed at 150 mV largely correspond to those arising from cations, single channel currents of 2.7 pA for $(6F10)_6$ and 0.65 pA for $(6F10{\cdot}IFT)_3$ indicate that a transmembrane pathway, made up of six vertically aligned crown ether units with an inter-chain distance of 4.8 Å, transports K^+ ions at a rate about 4 times as fast as that having only three such units of a wider separation distance of 9.6 Å. Alternatively, doubling the inter-chain distance between the ion binding sites while eliminating 50% of ion binding sites attenuates the ion transport ability by 76%.

Third, from the single channel currents recorded at different voltages (Figure 3c,d), the channel total opening times are 1.6 s out of a total recording time of 79.9 s for $(6F10)_6$ and 42.9 s out of 66.8 s for $(6F10{\cdot}IFT)_3$, roughly corresponding to channel opening probabilities of 2.0% for $(6F10)_6$ and 64.2% for $(6F10{\cdot}IFT)_3$. These drastically different channel opening probabilities fully validate our strategy of using sterically compatible groups (straight alkyl chains and *tert*-butyl groups) to create hetero-ensembles with high structural stability.

A novel calcein-based fluorescence assay recently developed by Gale was adopted in this work for evaluating Gly transport ability of various channels (Figure 4a).[74] The

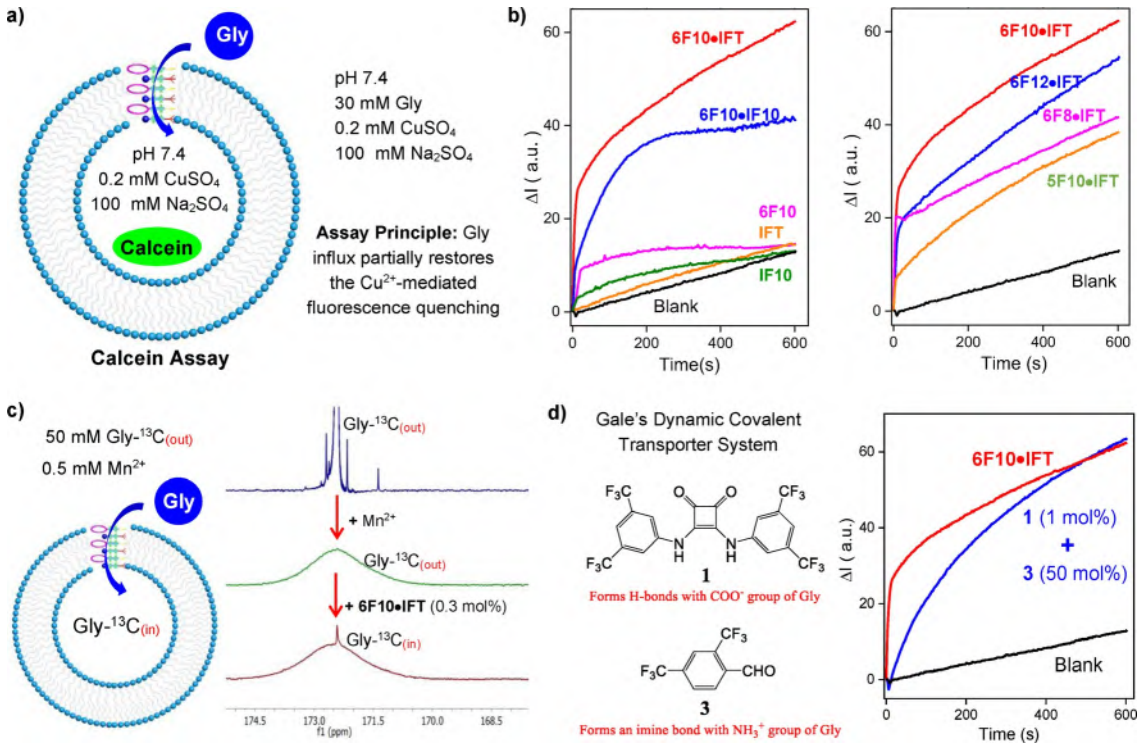

Figure 4. a) Illustration of amino acid-sensitive calcein assay for assessing the ability of amino acid transporters to transport glycine ($\lambda_{ex}=495$ nm, $\lambda_{em}=515$ nm). b) Glycine transport curves for various channels at 20 μM. c) ^{13}C NMR spectra that verify the glycine transport by hetero-channel $(6F10{\cdot}IFT)_3$. d) Glycine transport curves for $(6F10{\cdot}IFT)_3$ and Gale's dynamic covalent transporter system that employs **1** (1 mol%) and **3** (50 mol%).

principle of this assay is based on the competitive binding of intravesicular Cu^{2+} ions bound to calcein dye molecules by amino acids such as Gly transported into LUVs via synthetic amino acid transporters. Since it is Cu^{2+} ions, not amino acids, that quench the fluorescence of calcein dye, increasing removal of Cu^{2+} ions from calcein thereby increasingly restores the quenched calcein fluorescence, leading to enhancement in fluorescence (ΔI).

From data presented in Figure 4b, hetero-channel $(6F10{\cdot}IFT)_3$ evidently produces a significant fluorescence enhancement with respect to both $(6F10)_6$ and $(IFT)_6$, and this enhancement continues after 600 s. Interestingly, paring 6F10 with IF10 (obtained by replacing the *tert*-butyl group in IFT with a n-decyl group) forms hetero-channel $(6F10{\cdot}IF10)_3$ that is also able to transport Gly, but with transport activity starting to level off around 300 s. Paring IFT with either 6F12, having a longer dodecyl chain, or 6F8, having a shorter octyl chain, results in worse performance in Gly transport. Replacing 18-crown-6 group in 6F10 with the 15-crown-5 group generates 5F10, which similarly does not lead to improved Gly transport when paired with IFT. Taken together, hetero-channel $(6F10{\cdot}IFT)_3$ outperforms all the other combinations involving 6F8, 6F12, 5F10, and IF10.

^{13}C NMR spectra using ^{13}C labeled Gly (Gly-^{13}C) also used by Gale[74] provide more convincing evidence for Gly transport mediated by $(6F10{\cdot}IFT)_3$ (Figure 4c). The paramagnetic Mn^{2+} ions present in the extravesicular region exerts influences on the ^{13}C NMR signal from extravesicular Gly-^{13}C, but not intravesicular Gly-^{13}C signal. If transporter is able to facilitate influx of Gly-^{13}C, new ^{13}C signal is expected to be seen. Consistent with this expectation, we did observe a new discernable ^{13}C signal in the presence of 0.3 mol% $(6F10{\cdot}IFT)_3$, while prior to its addition, only a broad signal was obtained in the presence of 0.5 mM Cu^{2+} ions and 50 mM Gly-^{13}C.

Gale and his co-workers recently reported an elegant transporter system exploiting both H-bonds and dynamic covalent bond for Gly transport (Figure 4d).[74] After testing a number of molecules, the best combination involves squaramide molecule **1**, which forms H-bonds with the carboxylate group of Gly, and aldehyde molecule **3**, which forms a dynamic covalent imine bond with the ammonium group of Gly. The resultant tripartite complex 1·Gly·**3** is mostly hydrophobic and crosses the membrane by a simple diffusion process, with the fastest Gly influx occurring in the presence of 1 mol% **1** and 50 mol% **3**. Compared to Gale's dynamic transporter, hetero-channel $(6F10{\cdot}IFT)_3$ induces much faster Gly transport during the first 60 s, and achieves a similar overall performance over a duration of 600 s.

Following the same assay having 0.2 mM $CuSO_4$ in the extravesicular region (Figure 4a), we have examined another eleven amino acids. Results summarized in Figure 5a reveal six amino acids including Gly to be transportable. However, after or even before subtracting the background signals, the changes in fluorescence intensity of calcein for six amino acids all are negative (See Val, Ile, Met, Pro, Leu, and Phe in Figure 5a and the Supporting Information, Figure S3d, respectively). This is surprising given that such changes certainly are expected to be ≥ 0 even if channel $(6F10{\cdot}IFT)_3$ completely lacks an ability to transport these amino acids. The most plausible explanation is that, during the channel-mediated transport of amino acid, the electron-deficient iodide groups of the channel interact rather weakly with the carboxylate group of the amino acid, enabling it to interact

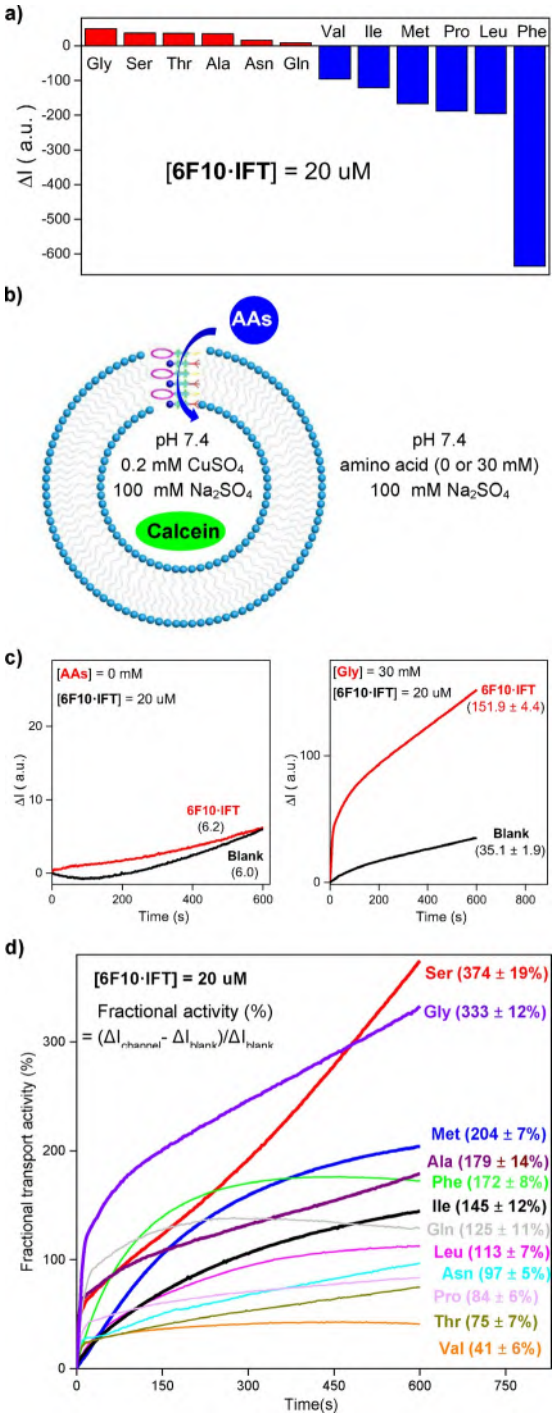

Figure 5. a) Net changes in fluorescence intensity of calcein using the assay conditions in Figure 4a. b) Illustration of new assay conditions, removing 0.2 mM $CuSO_4$ from the extravesicular region, with representative findings summarized in (c)–(e). Blank refers to the signals obtained in the absence of channel molecules. All data are the average of three independent measurements.

with and cause influx of Cu^{2+} ions to quench the fluorescence of calcein.

With the above reasoning in mind, we decided to remove 0.2 mM $CuSO_4$ from the extravesicular region (Figure 5b). Under these conditions, we further removed 30 mM amino acid to ascertain that the passive efflux of Cu^{2+} ions driven by the concentration gradient or mediated by channel $(6F10{\cdot}IFT)_3$ are maintained at the low levels (Figure 5c). It might be worth pointing out that, during the freeze/thaw cycles for LUV preparation, heating the lipid solution at 55 °C water bath for 2 minutes is very necessary to achieve low background signal shown in Figure 5c under the concentration gradient of Cu^{2+} ions that might lead to efflux of Cu^{2+}.

We then conducted systematic evaluations of 12 amino acids using the new assay shown in Figure 5b. In line with our expectations, channel $(6F10{\cdot}IFT)_3$ indeed displays measurable ability to transport all 12 amino acids (Figure 5d; Supporting Information, Figures S4, S5). To allow for straightforward and better comparison of the transport efficiencies for these amino acids, we defined the fractional activity as $(\Delta I_{channel}-\Delta I_{blank})/\Delta I_{blank})$ wherein $\Delta I_{channel}$ and ΔI_{blank} are changes in fluorescence signals obtained in the presence and absence of channel $(6F10{\cdot}IFT)_3$ (Figure 5e). Based on the calculated fractional activities, amino acid Ser stands out as the most preferred substrate, followed by Gly, Met and Ala, for transmembrane transport by $(6F10{\cdot}IFT)_3$.

Conclusion

Social self-sorting of functionalized peptidic scaffolds has been relatively rare and thus far difficult to achieve.[77] Herein, we have devised and demonstrated a novel bottom-up crystal structure-guided molecular strategy, allowing for social self-sorting to readily take place by pairing straight alkyl chains with sterically compatible *tert*-butyl groups. This process generates more stable hetero-oligomeric ensembles $(6F10{\cdot}IFT)_n$ from the corresponding homo-ensembles $(6F10)_n$ and $(IFT)_n$. The resultant alternatively arrayed cation-binding crown ethers and electron-deficient anion-binding iodide groups, which are aligned to the same side, exhibit better ion transport activities than the homo ensembles, and more importantly the three-in-one ability to transport cations, anions and zwitterionic amino acids. A broad application of this strategy to fabricating exciting peptide-based new functional materials of increasing complexity can be envisioned and expected.

Acknowledgements

This work was supported by College of Science, Hainan University.

Conflict of interest

The authors declare no conflict of interest.

Keywords: amino acid transporters · crown ethers · halogen bonds · supramolecular chemistry · synthetic ion channels

[1] D. R. Wise, C. B. Thompson, *Trends Biochem. Sci.* **2010**, *35*, 427–433.
[2] J. W. Locasale, *Nat. Rev. Cancer* **2013**, *13*, 572–583.
[3] C. F. Labuschagne, N. J. F. van den Broek, G. M. Mackay, K. H. Vousden, O. D. K. Maddocks, *Cell Rep.* **2014**, *7*, 1248–1258.
[4] Y. D. Bhutia, E. Babu, S. Ramachandran, V. Ganapathy, *Cancer Res.* **2015**, *75*, 1782.
[5] J. M. Weinberg, A. Bienholz, M. A. Venkatachalam, *Cell. Mol. Life Sci.* **2016**, *73*, 2285–2308.
[6] A. M. Hosios, V. C. Hecht, L. V. Danai, M. O. Johnson, J. C. Rathmell, M. L. Steinhauser, S. R. Manalis, M. G. Vander Heiden, *Dev. Cell* **2016**, *36*, 540–549.
[7] L. Bonfili, V. Cecarini, M. Cuccioloni, M. Angeletti, V. Flati, G. Corsetti, E. Pasini, F. S. Dioguardi, A. M. Eleuteri, *FEBS J.* **2017**, *284*, 1726–1737.
[8] P. Kandasamy, G. Gyimesi, Y. Kanai, M. A. Hediger, *Trends Biochem. Sci.* **2018**, *43*, 752–789.
[9] L. Lin, S. W. Yee, R. B. Kim, K. M. Giacomini, *Nat. Rev. Drug Discovery* **2015**, *14*, 543.
[10] E. Perland, R. Fredriksson, *Trends Pharm. Sci.* **2017**, *38*, 305–315.
[11] I. Tabushi, Y. Kuroda, K. Yokota, *Tetrahedron Lett.* **1982**, *23*, 4601–4604.
[12] A. J. Helsel, A. L. Brown, K. Yamato, W. Feng, L. H. Yuan, A. J. Clements, S. V. Harding, G. Szabo, Z. F. Shao, B. Gong, *J. Am. Chem. Soc.* **2008**, *130*, 15784–15785.
[13] S. Matile, A. Vargas Jentzsch, J. Montenegro, A. Fin, *Chem. Soc. Rev.* **2011**, *40*, 2453–2474.
[14] A. Vargas Jentzsch, A. Hennig, J. Mareda, S. Matile, *Acc. Chem. Res.* **2013**, *46*, 2791–2800.
[15] N. Sakai, S. Matile, *Langmuir* **2013**, *29*, 9031–9040.
[16] J. Montenegro, M. R. Ghadiri, J. R. Granja, *Acc. Chem. Res.* **2013**, *46*, 2955–2965.
[17] T. M. Fyles, *Acc. Chem. Res.* **2013**, *46*, 2847–2855.
[18] F. Otis, M. Auger, N. Voyer, *Acc. Chem. Res.* **2013**, *46*, 2934–2943.
[19] G. W. Gokel, S. Negin, *Acc. Chem. Res.* **2013**, *46*, 2824–2833.
[20] F. De Riccardis, I. Izzo, D. Montesarchio, P. Tecilla, *Acc. Chem. Res.* **2013**, *46*, 2781–2790.
[21] L. D. Mosgaard, T. Heimburg, *Acc. Chem. Res.* **2013**, *46*, 2966–2976.
[22] M. Barboiu, Y. Le Duc, A. Gilles, P.-A. Cazade, M. Michau, Y. M. Legrand, A. van der Lee, B. Coasne, P. Parvizi, J. Post, T. Fyles, *Nat. Commun.* **2014**, *5*, 4142.
[23] X. Wei, G. Zhang, Y. Shen, Y. Zhong, R. Liu, N. Yang, F. Y. Almkhaizim, M. A. Kline, L. He, M. Li, Z.-L. Lu, Z. Shao, B. Gong, *J. Am. Chem. Soc.* **2016**, *138*, 2749–2754.
[24] S. Negin, M. B. Patel, M. R. Gokel, J. W. Meisel, G. W. Gokel, *ChemBioChem* **2016**, *17*, 2153–2161.
[25] G. Su, M. Zhang, W. Si, Z.-T. Li, J.-L. Hou, *Angew. Chem. Int. Ed.* **2016**, *55*, 14678–14682; *Angew. Chem.* **2016**, *128*, 14898–14902.
[26] C. L. Ren, J. Shen, H. Q. Zeng, *J. Am. Chem. Soc.* **2017**, *139*, 12338–12341.
[27] C. Lang, X. Deng, F. Yang, B. Yang, W. Wang, S. Qi, X. Zhang, C. Zhang, Z. Dong, J. Liu, *Angew. Chem. Int. Ed.* **2017**, *56*, 12668–12671; *Angew. Chem.* **2017**, *129*, 12842–12845.
[28] C. Ren, F. Chen, R. J. Ye, Y. S. Ong, H. Lu, S. S. Lee, J. Y. Ying, H. Q. Zeng, *Angew. Chem. Int. Ed.* **2019**, *58*, 8034–8038; *Angew. Chem.* **2019**, *131*, 8118–8122.
[29] M. Barboiu, *Acc. Chem. Res.* **2018**, *51*, 2711–2718.

[30] R. J. Ye, C. L. Ren, J. Shen, N. Li, F. Chen, A. Roy, H. Q. Zeng, *J. Am. Chem. Soc.* **2019**, *141*, 9788 – 9792.
[31] F.-F. Shen, S.-Y. Dai, N.-K. Wong, S. Deng, A. S.-T. Wong, D. Yang, *J. Am. Chem. Soc.* **2020**, *142*, 10769 – 10779.
[32] P. Tripathi, L. Shuai, H. Joshi, H. Yamazaki, W. H. Fowle, A. Aksimentiev, H. Fenniri, M. Wanunu, *J. Am. Chem. Soc.* **2020**, *142*, 1680 – 1685.
[33] M. Debnath, S. Chakraborty, Y. P. Kumar, R. Chaudhuri, B. Jana, J. Dash, *Nat. Commun.* **2020**, *11*, 469.
[34] F. Chen, J. Shen, N. Li, A. Roy, R. J. Ye, C. L. Ren, H. Q. Zeng, *Angew. Chem. Int. Ed.* **2020**, *59*, 1440 – 1444; *Angew. Chem.* **2020**, *132*, 1456 – 1460.
[35] D. Bai, T. Yan, S. Wang, Y. Wang, J. Fu, X. Fang, J. Zhu, J. Liu, *Angew. Chem. Int. Ed.* **2020**, *59*, 13602 – 13607; *Angew. Chem.* **2020**, *132*, 13704 – 13709.
[36] L. Z. Zeng, H. Zhang, T. Wang, T. Li, *Chem. Commun.* **2020**, *56*, 1211 – 1214.
[37] N. Li, J. Shen, G. K. Ang, R. J. Ye, H. Q. Zeng, *CCS Chem.* **2021**, https://doi.org/10.31635/ccschem.31020.202000475.
[38] P. H. Schlesinger, R. Ferdani, J. Liu, J. Pajewska, R. Pajewski, M. Saito, H. Shabany, G. W. Gokel, *J. Am. Chem. Soc.* **2002**, *124*, 1848 – 1849.
[39] J. T. Davis, P. A. Gale, O. A. Okunola, P. Prados, J. C. Iglesias-Sánchez, T. Torroba, R. Quesada, *Nat. Chem.* **2009**, *1*, 138 – 144.
[40] C. R. Yamnitz, S. Negin, I. A. Carasel, R. K. Winter, G. W. Gokel, *Chem. Commun.* **2010**, *46*, 2838 – 2840.
[41] J. T. Davis, O. Okunola, R. Quesada, *Chem. Soc. Rev.* **2010**, *39*, 3843 – 3862.
[42] P. R. Brotherhood, A. P. Davis, *Chem. Soc. Rev.* **2010**, *39*, 3633 – 3647.
[43] N. Busschaert, L. E. Karagiannidis, M. Wenzel, C. J. E. Haynes, N. J. Wells, P. G. Young, D. Makuc, J. Plavec, K. A. Jolliffe, P. A. Gale, *Chem. Sci.* **2014**, *5*, 1118 – 1127.
[44] D. S. Kim, J. L. Sessler, *Chem. Soc. Rev.* **2015**, *44*, 532 – 546.
[45] T. Saha, M. S. Hossain, D. Saha, M. Lahiri, P. Talukdar, *J. Am. Chem. Soc.* **2016**, *138*, 7558 – 7567.
[46] T. Saha, A. Gautam, A. Mukherjee, M. Lahiri, P. Talukdar, *J. Am. Chem. Soc.* **2016**, *138*, 16443 – 16451.
[47] X. Wu, L. W. Judd, E. N. W. Howe, A. M. Withecombe, V. Soto-Cerrato, H. Li, N. Busschaert, H. Valkenier, R. Pérez-Tomás, D. N. Sheppard, Y.-B. Jiang, A. P. Davis, P. A. Gale, *Chem* **2016**, *1*, 127 – 146.
[48] S. Benz, M. Macchione, Q. Verolet, J. Mareda, N. Sakai, S. Matile, *J. Am. Chem. Soc.* **2016**, *138*, 9093 – 9096.
[49] B. P. Benke, P. Aich, Y. Kim, K. L. Kim, M. R. Rohman, S. Hong, I.-C. Hwang, E. H. Lee, J. H. Roh, K. Kim, *J. Am. Chem. Soc.* **2017**, *139*, 7432 – 7435.
[50] P. A. Gale, J. T. Davis, R. Quesada, *Chem. Soc. Rev.* **2017**, *46*, 2497 – 2519.
[51] C. L. Ren, F. Zeng, J. Shen, F. Chen, A. Roy, S. Zhou, H. Ren, H. Q. Zeng, *J. Am. Chem. Soc.* **2018**, *140*, 8817 – 8826.
[52] C. L. Ren, X. Ding, A. Roy, J. Shen, S. Zhou, F. Chen, S. F. Y. Li, H. Ren, Y. Y. Yang, H. Q. Zeng, *Chem. Sci.* **2018**, *9*, 4044 – 4051.
[53] L. Tapia, Y. Perez, M. Bolte, J. Casas, J. Sola, R. Quesada, I. Alfonso, *Angew. Chem. Int. Ed.* **2019**, *58*, 12465 – 12468; *Angew. Chem.* **2019**, *131*, 12595 – 12598.
[54] L. M. Lee, M. Tsemperouli, A. I. Poblador-Bahamonde, S. Benz, N. Sakai, K. Sugihara, S. Matile, *J. Am. Chem. Soc.* **2019**, *141*, 810 – 814.
[55] L. Yuan, J. Shen, R. J. Ye, F. Chen, H. Q. Zeng, *Chem. Commun.* **2019**, *55*, 4797 – 4800.
[56] S.-H. Park, S.-H. Park, E. N. W. Howe, J. Y. Hyun, L.-J. Chen, I. Hwang, G. Vargas-Zuñiga, N. Busschaert, P. A. Gale, J. L. Sessler, I. Shin, *Chem* **2019**, *5*, 2079 – 2098.
[57] H. Li, H. Valkenier, A. G. Thorne, C. M. Dias, J. A. Cooper, M. Kieffer, N. Busschaert, P. A. Gale, D. N. Sheppard, A. P. Davis, *Chem. Sci.* **2019**, *10*, 9663 – 9672.
[58] A. Roy, H. Joshi, R. J. Ye, J. Shen, F. Chen, A. Aksimentiev, H. Q. Zeng, *Angew. Chem. Int. Ed.* **2020**, *59*, 4806 – 4813; *Angew. Chem.* **2020**, *132*, 4836 – 4843.
[59] J. A. Malla, R. M. Umesh, S. Yousf, S. Mane, S. Sharma, M. Lahiri, P. Talukdar, *Angew. Chem. Int. Ed.* **2020**, *59*, 7944 – 7952; *Angew. Chem.* **2020**, *132*, 8018 – 8026.
[60] W.-L. Huang, X.-D. Wang, Y.-F. Ao, Q.-Q. Wang, D.-X. Wang, *J. Am. Chem. Soc.* **2020**, *142*, 13273 – 13277.
[61] M. Barboiu, A. Gilles, *Acc. Chem. Res.* **2013**, *46*, 2814 – 2823.
[62] B. Gong, Z. Shao, *Acc. Chem. Res.* **2013**, *46*, 2856 – 2866.
[63] H. Q. Zhao, S. Sheng, Y. H. Hong, H. Q. Zeng, *J. Am. Chem. Soc.* **2014**, *136*, 14270 – 14276.
[64] W. Si, P. Xin, Z.-T. Li, J.-L. Hou, *Acc. Chem. Res.* **2015**, *48*, 1612 – 1619.
[65] Y.-x. Shen, W. Si, M. Erbakan, K. Decker, R. De Zorzi, P. O. Saboe, Y. J. Kang, S. Majd, P. J. Butler, T. Walz, A. Aksimentiev, J.-l. Hou, M. Kumar, *Proc. Natl. Acad. Sci. USA* **2015**, *112*, 9810 – 9815.
[66] Y. P. Huo, H. Q. Zeng, *Acc. Chem. Res.* **2016**, *49*, 922 – 930.
[67] J. Shen, J. Fan, R. J. Ye, N. Li, Y. Mu, H. Q. Zeng, *Angew. Chem. Int. Ed.* **2020**, *59*, 13328 – 13334; *Angew. Chem.* **2020**, *132*, 13430 – 13436.
[68] Z.-J. Yan, D. Wang, Z. Ye, T. Fan, G. Wu, L. Deng, L. Yang, B. Li, J. Liu, T. Ma, C. Dong, Z.-T. Li, L. Xiao, Y. Wang, W. Wang, J.-L. Hou, *J. Am. Chem. Soc.* **2020**, *142*, 15638 – 15643.
[69] J. Shen, R. J. Ye, A. Romanies, A. Roy, F. Chen, C. L. Ren, Z. Liu, H. Q. Zeng, *J. Am. Chem. Soc.* **2020**, *142*, 10050 – 10058.
[70] W. Song, H. Joshi, R. Chowdhury, J. S. Najem, Y.-x. Shen, C. Lang, C. B. Henderson, Y.-M. Tu, M. Farell, M. E. Pitz, C. D. Maranas, P. S. Cremer, R. J. Hickey, S. A. Sarles, J.-l. Hou, A. Aksimentiev, M. Kumar, *Nat. Nanotechnol.* **2020**, *15*, 73 – 79.
[71] A. Roy, J. Shen, H. Joshi, W. Song, Y.-M. Tu, R. J. Ye, N. Li, C. L. Ren, M. Kumar, A. Aksimentiev, H. Q. Zeng, *Chemrxiv* **2020**, https://doi.org/10.26434/chemrxiv.12860981.v12860981.
[72] Y. Zhao, H. Cho, L. Widanapathirana, S. Zhang, *Acc. Chem. Res.* **2013**, *46*, 2763 – 2772.
[73] L. Chen, W. Si, L. Zhang, G. Tang, Z. T. Li, J. L. Hou, *J. Am. Chem. Soc.* **2013**, *135*, 2152 – 2155.
[74] X. Wu, N. Busschaert, N. J. Wells, Y.-B. Jiang, P. A. Gale, *J. Am. Chem. Soc.* **2015**, *137*, 1476 – 1484.
[75] A. V. Jentzsch, D. Emery, J. Mareda, S. K. Nayak, P. Metrangolo, G. Resnati, N. Sakai, S. Matile, *Nat. Commun.* **2012**, *3*, 905.
[76] F. Otis, C. Racine-Berthiaume, N. Voyer, *J. Am. Chem. Soc.* **2011**, *133*, 6481 – 6483.
[77] K. L. Morris, L. Chen, J. Raeburn, O. R. Sellick, P. Cotanda, A. Paul, P. C. Griffiths, S. M. King, R. K. O'Reilly, L. C. Serpell, D. J. Adams, *Nat. Commun.* **2013**, *4*, 1480.

Manuscript received: January 31, 2021
Revised manuscript received: March 22, 2021
Accepted manuscript online: March 23, 2021
Version of record online: May 5, 2021

